# An Efficient Wavelength Converter Exploiting a Grating-Based Saw-Tooth Pulse Shaper

F. Parmigiani, M. Ibsen, T. T. Ng, L. Provost, P. Petropoulos, and D. J. Richardson

***Abstract*—We experimentally demonstrate the generation of picosecond triangular optical pulses using a superstructured fiber Bragg grating and show experimentally that use of this pulse shape can provide a three-fold improvement in conversion efficiency relative to the use of Gaussian pulses with similar pulsewidths when used in a wavelength conversion scheme based on self-phase modulation and subsequent offset filtering.**

***Index Terms*—Fiber Bragg grating, highly nonlinear fiber (HNLF), optical Kerr effect, optical pulse shaping, self-phase modulation (SPM).**

## I. Introduction

THE relentless increase in data traffic within optical networks is driving the requirement for increased capacity and bit rates within access, metropolitan, and core networks. As a result there is growing acceptance of the need to develop all-optical processing techniques to help increase the transparency of the network and to reduce the electrical processing requirements. The development of new techniques to monitor and manipulate the detailed shape and characteristics of the optical signals is, therefore, becoming progressively more important.

Superstuctured fiber Bragg grating (SSFBG) technology, which allows the development of optical filters with accurately controlled frequency and phase responses of almost arbitrary complexity in a single, continuous grating structure (see [1] for example), provides an extremely powerful tool for advanced photonic applications that require manipulation of the precise shape of short optical pulses in both the time and frequency domains. Pulse shaping with SSFBGs is a purely passive and linear process and relies upon designing and fabricating gratings with engineered spectral responses that transform pulses of a well-specified form incident upon the grating into a given desired output pulse shape.

This functionality allows one to consider developing pulse processing systems in which the shape of the input pulses is optimized to enhance the overall performance of the system. Using this all-fiberized polarization insensitive linear technique, we have successfully demonstrated the application of pulse reshaping for optical regeneration/retiming [2], [3], demultiplexing [4], and optimal pulse compression [5].

Manuscript received April 12, 2008; revised May 21, 2008. This work was supported in part by STREP TRIUMPH (IST-027638). The work of M. Ibsen was supported by a Royal Society University Research Fellowship.

The authors are with the Optoelectronics Research Centre, University of Southampton, Highfield, Southampton SO17 1BJ, U.K. (e-mail: frp@orc.soton.ac.uk).

Color versions of one or more of the figures in this letter are available online at http://ieeexplore.ieee.org.

Digital Object Identifier 10.1109/LPT.2008.927887

In this letter, we demonstrate a simple, cost-effective, all-optical wavelength converter based on self-phase modulation (SPM) and offset filtering which is particularly suited for applications in which the required wavelength shift is modest [6]. We then study and experimentally demonstrate that a saw-tooth-shaped input signal (asymmetric triangular pulse) is the optimal choice of pulse shape to enhance the efficiency of such a system. Note that this pulse shape, which can be used to generate constant wavelength shifts for signals through both SPM and cross-phase modulation effects, is of great interest for various other applications. Amongst these, optical time-division add–drop multiplexing is an important example [7], [8].

## II. SSFBG Design and Corresponding Pulse Shape Characterization

We generate picosecond triangular pulses using our SSFBG-based pulse-shaping technology. We produce asymmetric triangular pulses $\sim$10 ps [full-width at half-maximum (FWHM)], where the rising edge of the triangular shape is designed to be four times wider than the falling edge.

The corresponding spatial refractive index modulation envelope profile of the SSFBG, designed to work optimally with an input transform-limited $\sim$1.3-ps Gaussian pulse (Input 1), and its corresponding simulated (dashed line) and measured (solid line) spectral response are shown in Fig. 1(a) and (b), respectively. The peak reflectivity of the grating is 25%, corresponding to a modulation index of $4e-4$. We can accommodate 13 spectral lobes within the available 6-nm spectral bandwidth, while the total length of the grating is about 3 mm. Note that in our actual experiments we used broader pulses at the SSFBG input (Input 2 $\sim$2-ps $\text{sech}^2$ pulses) meaning that the shaped pulses are expected to have the same FWHM but smoother edges than targeted. We performed a full (phase and amplitude) characterization of the shaped pulses using a linear frequency-resolved optical gating (l-FROG) technique and confirmed these predictions. In Fig. 1(c), we plot the temporal profile of the measured triangular pulse and its corresponding chirp, while Fig. 1(d) shows that the retrieved spectrum agrees well with that measured. As a reference, a measured Gaussian pulse with similar FWHM is also plotted in Fig. 1(c). Furthermore, as expected, the calculated time derivative of the measured intensity profile is shown to be constant across the slower rising edge of the pulse [Fig. 1(e)].

## III. Principle of Operation

The proposed wavelength conversion scheme is based on the well-known frequency shifting effect of SPM in a highly non-

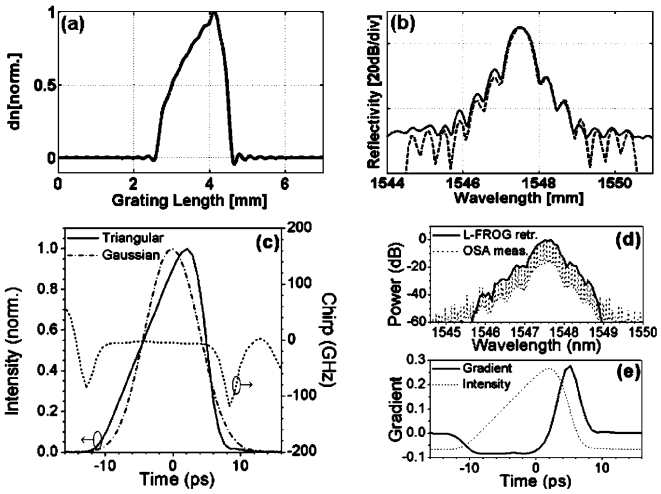


Fig. 1. (a) Refractive index modulation profile of the SSFBG. (b) Corresponding simulated (dashed line) and measured (solid line) spectral responses. (c) Measured intensity (solid line) and chirp profile (dotted line) of the shaped pulse. A Gaussian profile of a similar FWHM is also shown for comparison (dotted–dashed line). (d) Measured and retrieved triangular spectra. (e) Measured triangular intensity profile and a calculation of its gradient.

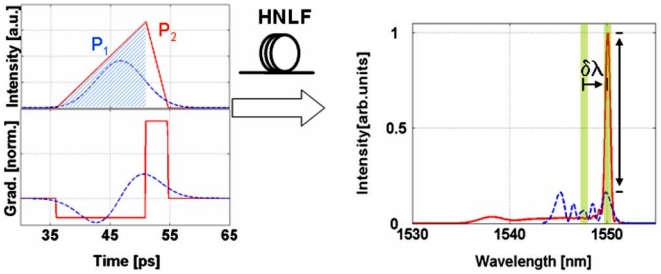


Fig. 2. Illustration as to how saw-tooth and Gaussian temporal pulse shapes spectrally broaden within an HNLF. The corresponding gradients are reported.

linear fiber (HNLF) (see for example [7] and [8]), which can be mathematically described by

$$\delta\omega(T) = -\frac{\partial\phi_{\rm NL}}{\partial T} = -\gamma P_o L_{\rm eff}\frac{\partial|U(T-\Delta T)|^2}{\partial T} \qquad (1)$$

where $\delta\omega(T)$ is the SPM frequency shift induced on the signal itself, $\gamma$ and $L_{\rm eff}$ are the nonlinear coefficient and effective length of the fiber, respectively, $P_o$ is the signal peak power, and $U(T)$ is its corresponding normalized pulse envelope. Equation (1) shows that the leading (trailing) edge of a saw-tooth pulse, which has a linear slope, induces a constant red (blue) frequency shift in its spectrum due to SPM. This implies that all the signal spectral components are up- or down-shifted with respect to the initial central wavelength, with minimum additional spectral broadening.

Furthermore, because the saw-tooth wave has an asymmetric shape, the spectral intensity evolution is also asymmetric, with the smoother leading edge experiencing less frequency shift than the sharper trailing edge (Fig. 2). However, because the energy associated with the smoother leading edge (dashed area in Fig. 2) is greater than that associated with the trailing edge, the red-shifted spectral peak is higher than that of the blue-shifted peak. This is clearly shown in Fig. 2, where the detailed simulated spectral broadening of a triangular pulse is compared to that of a conventional Gaussian pulse of a similar FWHM. Nevertheless, note that a lower input power is required for a Gaussian pulse than a triangular pulse to achieve the same peak wavelength shift due to the steeper gradients associated with a Gaussian intensity profile (see (1) and Fig. 2).

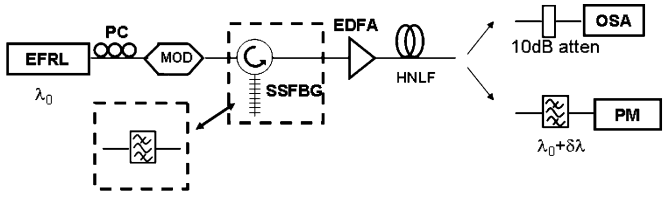


Fig. 3. Experimental setup. MOD: amplitude modulator; EDFA: erbium-doped fiber amplifier; PM: power meter; OSA: optical spectrum analyzer.

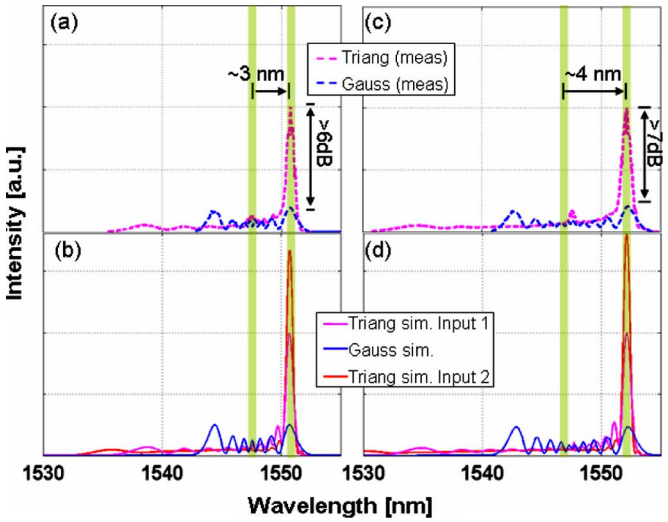


Fig. 4. (a), (b) Measured spectra of the triangular (pink dashed line) and Gaussian (blue dashed line) pulses at different input average powers and corresponding simulation spectra for the same input pulse shapes/widths. (c), (d) Spectral broadening of the triangular shape when Input 2 enters the SSFBG is also reported.

## IV. Experimental Setup and Results

The experimental setup of the wavelength converter is depicted in Fig. 3. A mode-locked erbium-doped fiber ring laser (EFRL) operating at ∼1547.6 nm is used to generate ∼2-ps sech$^2$ pulses at a repetition rate of 10 GHz. The signal is then amplitude modulated by a $2^{31}-1$-long pseudorandom bit sequence and shaped into ∼10-ps asymmetric triangular pulses [see Fig. 2(c)] via the grating. The signal is then amplified before being fed into 310 m of HNLF, which exhibits a dispersion of −0.31 ps/nm/km at 1550 nm and a nonlinear coefficient of ∼19 W/km. Alternatively, Gaussian pulses of ∼10 ps were generated by replacing the SSFBG with a narrowband filter with a Gaussian transmission profile to obtain ∼10-ps Gaussian pulses [Fig. 2(c)]. We started by propagating the triangular pulses along the HNLF and studied the spectral broadening evolution for different input power levels. Fig. 4(a) and (c) shows two experimentally obtained examples of spectra at the output of the

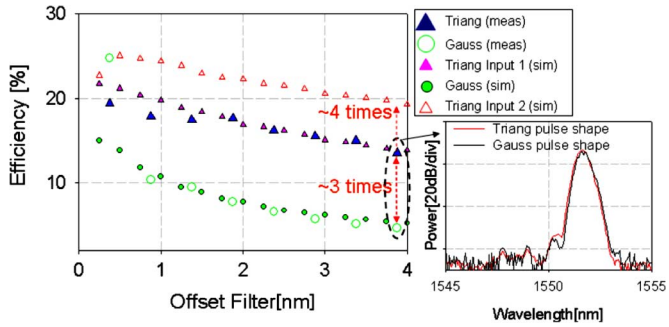


Fig. 5. Efficiency of the measured (simulated) triangular, when Inputs 1 and 2 enter the SSFBG, and Gaussian pulse shape as a function of the offset filter position. Corresponding simulated efficiency of the triangular pulse, when Input 2 enters the SSFBG, is also reported. Inset: Corresponding measured filtered spectra.

HNLF for wavelength shifts of ∼3 and ∼4 nm, which correspond to input average powers of ∼26 and 27.5 dBm, respectively. These results closely follow the numerical simulations reported in Fig. 4(b) and (d), where the incoming signal, labelled as Input 2, is shaped by the SSFBG.

Using Gaussian pulses lower average input powers (now ∼23 and ∼25 dBm, respectively) were required to achieve the same wavelength shifts as expected. The corresponding spectra broaden symmetrically about the original wavelength and complex multilobed spectra are obtained. This is clearly shown in Fig. 4(a) and (c), where it can be appreciated that the spectral peaks of the triangular pulses are typically more than 6–7 dB higher than the corresponding Gaussian peaks, in accordance with the simulated spectra [Fig. 4(b) and (d)]. As a reference, we simulated the spectral broadening of pulses conforming to the SSFBG design specification (Input 1) for the same wavelength shifts. As expected, stronger spectral peaks are achieved at the specific wavelengths due to the steeper edges of this triangular shape at the expense of higher input powers for the same wavelength shift (∼0.5 dB higher).

We then incorporated an offset filter (∼0.5-nm bandwidth) after the HNLF to convert the signal to the desired wavelength. The inset of Fig. 5 shows two examples of measured filtered spectra for the two temporal intensity profiles. The resulting pulse shape is determined mainly by the filter characteristics. Fig. 5 shows the measured conversion efficiency for the various pulse shapes as a function of the offset filter position. This is calculated as the ratio between the average signal powers after the offset filter relative to that at the input to the HNLF. As expected for this kind of wavelength converter, the efficiency decreases as the detuning of the filter is increased, closely following the trend anticipated from the simulations. Compared to Gaussian pulses, triangular pulses show an increased efficiency as the offset filter position is moved away from the wavelength of the input signal reaching an experimental three-fold improvement for a wavelength shift of ∼4 nm. This efficiency would be increased to a factor of four for the largest detuning of the filter if Input 1 was used (Fig. 5).

## V. Conclusion

We have experimentally demonstrated the generation of saw-tooth pulses using pulse shaping in an SSFBG. This intensity profile is very interesting for applications that can exploit the corresponding constant time derivative profile of such pulses. As a first example, we have shown the enhanced performance of a wavelength converter based on SPM in HNLF and subsequent offset filtering. An efficiency increase up to three times for a wavelength shifting of ∼4 nm was experimentally reported when compared to conventional pulse shapes, while simulations show that a four-fold increase would have been achieved with a proper choice of input pulse duration.

## Acknowledgment

The authors acknowledge The Furukawa Electric Company, Japan, for the loan of the HNLF.

## References

[1] P. Petropoulos, M. Ibsen, A. D. Ellis, and D. J. Richardson, "Rectangular pulse generation based on pulse reshaping using superstructured fiber Bragg grating," *J. Lightw. Technol.*, vol. 19, no. 5, pp. 746–752, May 2001.

[2] F. Parmigiani, L. K. Oxenlowe, M. Galili, M. Ibsen, D. Zibar, P. Petropoulos, D. J. Richardson, A. T. Clausen, and P. Jeppesen, "All-optical 160 Gbit/s RZ data retiming system incorporating a pulse shaping fibre Bragg grating," in *ECOC*, Berlin, Germany, 2007, Paper Tu 5.3.1.

[3] F. Parmigiani, P. Petropoulos, M. Ibsen, and D. J. Richardson, "Pulse retiming based on XPM using parabolic pulses formed in a fiber Bragg grating," *IEEE Photon. Technol. Lett.*, vol. 18, no. 7, pp. 829–831, Apr. 1, 2006.

[4] J. H. Lee, P. C. Teh, P. Petropoulos, M. Ibsen, and D. J. Richardson, "All optical modulation and demultiplexing systems with significant timing jitter tolerance through incorporation of pulse-shaping fiber Bragg gratings," *IEEE Photon. Technol. Lett.*, vol. 14, no. 2, pp. 203–205, Feb. 2002.

[5] F. Parmigiani, C. Finot, K. Mukasa, M. Ibsen, M. A. F. Roelens, P. Petropoulos, and D. J. Richardson, "Ultra-flat SPM-broadened spectra in a highly nonlinear fiber using parabolic pulses formed in a fiber Bragg grating," *Opt. Express*, vol. 14, no. 17, pp. 7617–7622, 2006.

[6] S. Watanabe, F. Futami, R. Okabe, Y. Takita, S. Ferber, R. Ludwig, C. Schubert, C. Schmidt, and H. G. Weber, "160 Gb/s Optical 3R-Regenerator in fiber transmission experiment," in *Proc. OFC*, Atlanta, GA, 2003, Paper PD16-1.

[7] J. Li, B.-E. Olsson, M. Karlsson, and P. A. Andrekson, "OTDM add-drop multiplexer based on xpm-induced wavelength shifting in highly nonlinear fiber," *J. Lightw. Technol.*, vol. 23, no. 9, pp. 2654–2661, Sep. 2005.

[8] B.-E. Olsson, P. Ohlen, L. Rau, and D. J. Blumenthal, "A simple and robust 40-Gb/s wavelength converter using fiber cross-phase modulation and optical filtering," *IEEE Photon. Technol. Lett.*, vol. 12, no. 7, pp. 846–848, Jul. 2000.